

MASTER

PROJECTILE CHARGE STATE DEPENDENCE OF M-SHELL IONIZATION OF Au, Pb, Bi and U BY 1.42-MeV/amu FLUORINE IONS\*

R. Mehta, J.L. Duggan, F.D. McDaniel, M.C. Andrews  
Department of Physics  
North Texas State University\*\*  
Denton, TX 76203

and  
R.M. Wheeler and R.P. Chaturvedi  
Department of Physics  
SUNY at Cortland  
Cortland, N.Y. 13045

and  
P.D. Miller  
Physics Division  
Oak Ridge National Laboratory†  
Oak Ridge, TN 37830

and  
G. Lapicki  
Department of Chemistry and Physics  
Northwestern State University of Louisiana  
Natchitoches, LA 71457

151 4327

451 1328

DISCLAIMER  
This book was prepared as an account of work sponsored by an agency of the United States Government. Neither the United States Government nor any agency thereof, nor any of their employees, makes any warranty, expressed or implied, or assumes any legal liability or responsibility for the accuracy, completeness, or usefulness of any information, apparatus, product, or process disclosed, or represents that its use would not infringe privately owned rights. Reference herein to any specific commercial product, process or service by trade name, trademark, manufacturer, or otherwise, does not necessarily constitute or imply its endorsement, recommendation, or favoring by the United States Government or any agency thereof. The views and opinions of authors expressed herein do not necessarily state or reflect those of the United States Government or any agency thereof.

Summary

The present study was undertaken to determine the direct ionization and electron capture contributions to vacancy production in the M-shells of  $^{79}\text{Au}$ ,  $^{82}\text{Pb}$ ,  $^{83}\text{Bi}$  and  $^{92}\text{U}$  for incident  $^{19}\text{F}$  ions. M-shell x-ray production cross sections have been measured for 1.42-MeV/amu  $^{19}\text{F}^q$  ions for  $q=4,5,6,8,9$ . Enhancements in the target x-ray production cross sections were observed for projectiles with one and two K-shell vacancies over those without K-shell vacancies. Direct ionization and electron capture contributions to the vacancy production were extracted from the data and compared to the plane wave Born approximation<sup>1,2</sup> and to the Oppenheimer-Brinkman-Kramers<sup>3,4</sup> calculations of Nikolaev<sup>5</sup>, respectively.

Introduction

In the past few years new interest has emerged in the study of inner-shell vacancy production in heavy ion-atom collisions. At high velocities, the two primary mechanisms involved are the direct ionization to the continuum (DI) and the electron capture by the projectile (EC).

Calculations of the ionization cross sections for the K- and L-shells have been performed in the plane wave Born approximation (PWBA)<sup>7</sup>. Recently, Basbas et al<sup>8</sup> have presented a perturbed stationary state formalism (PSS) which includes the effects of polarization and increased binding. These calculations which also include Coulomb deflection of the ion provide good agreement with DI data of McDaniel et al<sup>9</sup>.

The electron capture contribution to the target vacancy production cross section can be calculated for heavy ions by several different theoretical approaches. Reading et al<sup>10</sup>, Lin et al<sup>11</sup>, Lapicki and Losonsky<sup>12</sup>, Lapicki and McDaniel<sup>13</sup>, and others<sup>14,15</sup> have proposed models to explain EC.

Lapicki and coworkers<sup>12,13</sup> have recently developed a theoretical approach which, although expressed in

terms of Oppenheimer, Brinkman, Kramers<sup>3,4</sup> Nikolaev<sup>5</sup> (OBK-N) formulas for convenience, goes beyond the OBK-N approximation since it accounts for the perturbed stationary state (PSS) and relativistic effects. These calculations have been made primarily for the K-shell to K-shell charge transfer<sup>6</sup> as have other theoretical approaches that exist at this time.

Gray et al<sup>16</sup> have also determined the DI and EC contributions to vacancy production for the K-shell for a range of ion-target combinations. For convenience, they have applied semi-empirical scaling factors to the OBK-N to determine the EC cross sections for their experimental data.

McDaniel and co-workers<sup>9,17</sup> investigated the K-shell ionization by  $^{19}\text{F}$  ions and the L-shell ionization by  $^{19}\text{F}$  and  $^{28}\text{Si}$  ions. The CPSS theory of Basbas et al<sup>8</sup> combined with EC theory of Lapicki and McDaniel<sup>13</sup> was in excellent agreement with their study for the K-shell<sup>9</sup>. Electron capture measurements for the L-shell were also found to be in excellent agreement with the EC theory of Lapicki and McDaniel<sup>13</sup>.

In the present work, we are extending the above investigation of McDaniel et al<sup>9,17</sup> to the M-shell. We have measured the M-shell x-ray production cross sections for thin solid targets of  $^{79}\text{Au}$ ,  $^{82}\text{Pb}$ ,  $^{83}\text{Bi}$  and  $^{92}\text{U}$  for incident 1.42 MeV/amu  $^{19}\text{F}$  ions.

The EC cross section are inferred by comparing the measured M-shell x-ray production cross sections for projectiles with one or two K-shell vacancies to the average M-shell x-ray production cross section for projectiles without K-shell vacancies.

The only theoretical ionization cross sections calculations presently available for the M-shell are the PWBA<sup>1-3</sup> for DI and the OBK-N<sup>6</sup> for EC. These theoretical calculations are used to make comparisons with the experimental data in the present study.

Experimental Procedure and Data Analysis

A 1.42 MeV/amu beam of  $^{19}\text{F}^q$  ions was obtained from the En Tandem Van De Graaff accelerator at Oak Ridge National Laboratory. The beam was passed through a stripper foil and was magnetically analyzed for charge states  $q=4,5,6,8$  or  $9$ . After collimation, the ion beam was incident on thin solid targets inclined at 60 degrees to the incident beam direction.

\* Travel to ORNL is provided by ORAU  
\*\* Supported in part by the Robert A. Welch Foundation, The Research Corporation, and the NTSU Organized Research Fund. Acknowledgement is made to the donors of the Petroleum Research Fund, administered by the American Chemical Society, for partial support of this research.  
† Supported by DOE, Division of Basic Sciences, Contract No. W-7405-ENG-26 with Union Carbide Corp.

MSW

PROJECTILE CHARGE STATE DEPENDENCE OF M-SHELL  
IONIZATION OF Au, Pb, Bi and U BY 1.42-MeV/amu FLUORINE IONS\*

C  
CONF-801111--55

DE82 003967

R. Mehta, J.L. Duggan, F.D. McDaniel, M.C. Andrews  
Department of Physics  
North Texas State University\*\*  
Denton, TX 76203

and  
R.M. Wheeler and R.P. Chaturvedi  
Department of Physics  
SUNY at Cortland  
Cortland, N.Y. 13045

and  
P.D. Miller  
Physics Division  
Oak Ridge National Laboratory†  
Oak Ridge, TN 37830

and  
G. Lapicki  
Department of Chemistry and Physics  
Northwestern State University of Louisiana  
Natchitoches, LA 71457

DISCLAIMER

This work was prepared as an account of work sponsored by the United States Government. Therefore, neither the United States Government nor any agency thereof, nor any of their employees, makes any warranty, expressed or implied, or assumes any legal liability or responsibility for the accuracy, completeness, or usefulness of any information, apparatus, product, or process disclosed, or represents that it would necessarily benefit the general public. Reference herein to any specific commercial product, process, or service by its trade name, trademark, manufacturer, or otherwise, does not constitute an endorsement or recommendation for its use by the United States Government. The views and opinions of authors expressed herein do not necessarily state or reflect those of the United States Government or any agency thereof.

Summary

The present study was undertaken to determine the direct ionization and electron capture contributions to vacancy production in the M-shells of  $^{79}\text{Au}$ ,  $^{82}\text{Pb}$ ,  $^{83}\text{Bi}$  and  $^{92}\text{U}$  for incident  $^{19}\text{F}$  ions. M-shell x-ray production cross sections have been measured for 1.42-MeV/amu  $^{19}\text{F}^{q+}$  ions for  $q=4,5,6,8,9$ . Enhancements in the target x-ray production cross sections were observed for projectiles with one and two K-shell vacancies over those without K-shell vacancies. Direct ionization and electron capture contributions to the vacancy production were extracted from the data and compared to the plane wave Born approximation<sup>1-3</sup> and to the Oppenheimer-Brinkman-Kramers<sup>4,5</sup> calculations of Nikolaev<sup>6</sup>, respectively.

Introduction

In the past few years new interest has emerged in the study of inner-shell vacancy production in heavy ion-atom collisions. At high velocities, the two primary mechanisms involved are the direct ionization to the continuum (DI) and the electron capture by the projectile (EC).

Calculations of the ionization cross sections for the K- and L-shells have been performed in the plane wave Born approximation (PWBA)<sup>7</sup>. Recently, Basbas et al<sup>8</sup> have presented a perturbed stationary state formalism (PSS) which includes the effects of polarization and increased binding. These calculations which also include Coulomb deflection of the ion provide good agreement with DI data of McDaniel et al<sup>9</sup>.

The electron capture contribution to the target vacancy production cross section can be calculated for heavy ions by several different theoretical approaches. Reading et al<sup>10</sup>, Lin et al<sup>11</sup>, Lapicki and Losonsky<sup>12</sup>, Lapicki and McDaniel<sup>13</sup>, and others<sup>14,15</sup> have proposed models to explain EC.

Lapicki and coworkers<sup>12,13</sup> have recently developed a theoretical approach which, although expressed in

terms of Oppenheimer, Brinkman, Kramers<sup>4,5</sup> Nikolaev<sup>6</sup> (OBK-N) formulas for convenience, goes beyond the OBK-N approximation since it accounts for the perturbed stationary state (PSS) and relativistic effects. These calculations have been made primarily for the K-shell to K-shell charge transfer<sup>5</sup> as have other theoretical approaches that exist at this time.

Gray et al<sup>16</sup> have also determined the DI and EC contributions to vacancy production for the K-shell for a range of ion-target combinations. For convenience, they have applied semi-empirical scaling factors to the OBK-N to determine the EC cross sections for their experimental data.

McDaniel and co-workers<sup>9,17</sup> investigated the K-shell ionization by  $^{28}\text{Si}$  ions and the L-shell ionization by  $^{19}\text{F}$  and  $^{28}\text{Si}$  ions. The CPSS theory of Basbas et al<sup>8</sup> combined with EC theory of Lapicki and McDaniel<sup>13</sup> was in excellent agreement with their study for the K-shell<sup>9</sup>. Electron capture measurements for the L-shell were also found to be in excellent agreement with the EC theory of Lapicki and McDaniel<sup>13</sup>.

In the present work, we are extending the above investigation of McDaniel et al<sup>9,17</sup> to the M-shell. We have measured the M-shell x-ray production cross sections for thin solid targets of  $^{79}\text{Au}$ ,  $^{82}\text{Pb}$ ,  $^{83}\text{Bi}$  and  $^{92}\text{U}$  for incident 1.42 MeV/amu  $^{19}\text{F}$  ions.

The EC cross section are inferred by comparing the measured M-shell x-ray production cross sections for projectiles with one or two K-shell vacancies to the average M-shell x-ray production cross section for projectiles without K-shell vacancies.

The only theoretical ionization cross sections calculations presently available for the M-shell are the PWBA<sup>1-3</sup> for DI and the OBK-N<sup>6</sup> for EC. These theoretical calculations are used to make comparisons with the experimental data in the present study.

Experimental Procedure and Data Analysis

A 1.42 MeV/amu beam of  $^{19}\text{F}^{q+}$  ions was obtained from the En Tandem Van De Graaff accelerator at Oak Ridge National Laboratory. The beam was passed through a stripper foil and was magnetically analyzed for charge states  $q=4,5,6,8$  or  $9$ . After collimation, the ion beam was incident on thin solid targets inclined at 60 degrees to the incident beam direction.

\* Travel to ORNL is provided by ORAU

\*\* Supported in part by the Robert A. Welch Foundation, The Research Corporation, and the NISU Organized Research Fund. Acknowledgement is made to the donors of the Petroleum Research Fund, administered by the American Chemical Society, for partial support of this research.

† Supported by DOE, Division of Basic Sciences, Contract No. W-7405-ENG-26 with Union Carbide Corp.

MFW

An ORTEC Si(Li) detector, with a resolution of 155 eV at 5.9 keV, was positioned at 90 degrees to the incident beam direction to detect the x-rays from the target.

Fig. 1 shows an M-shell x-ray spectrum of  $^{79}\text{Au}$  for incident  $^{19}\text{F}$  ions. There are four major resolved peaks  $M_{\zeta_1\zeta_2}$ ,  $M\alpha\beta$ ,  $M\gamma$  and  $M_2-N_4$  (also labeled with  $M_1-N_2$  and  $M_3-O_4$ , which are the transitions included in that peak).  $M\gamma$  appears as a shoulder on the high energy side of  $M\alpha\beta$  while  $M_{\zeta_1\zeta_2}$  and  $M_2-N_4$  are better resolved.

To determine the yield under a peak, a background of a second order polynomial was subtracted from the spectrum. A peakfitting program, which generates Gaussian peaks (shown by dashed curves in the figure), is used to determine the best fitting parameters. Due to non-uniqueness of the solution for these parameters, uncertainty is introduced in the yields which ranges from 1 to 6 percent.

A theoretical curve for the absolute efficiency of the Si(Li) detector was calculated by determining the attenuation of x-rays in the Be window, the Au contact layer and the Si dead layer<sup>19</sup>. This curve was normalized to the measured efficiency points at x-ray energies of 3.3 keV and above.

A movable surface barrier detector counted the scattered particles. M-shell x-ray production cross sections were obtained by normalizing the x-ray yield to the Rutherford yield of scattered particles.

The targets, which were made by vacuum evaporation and deposition of the target element on  $\sim 20 \mu\text{g}/\text{cm}^2$  carbon backings, were bombarded with 1 and 2 MeV proton beams to determine the target thicknesses.

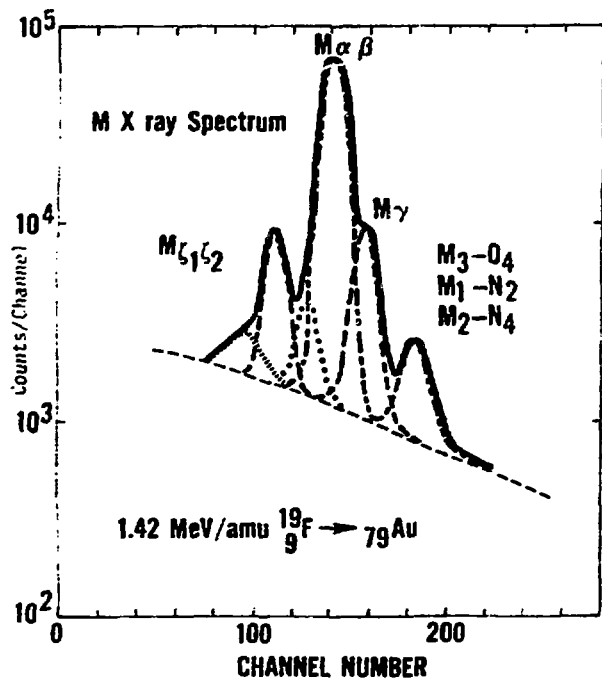


Fig. 1 An M x-ray spectrum of  $^{79}\text{Au}$  for incident 1.42 MeV/amu  $^{19}\text{F}$  ions is shown here. The spectrum shows four major peaks labeled  $M_{\zeta_1\zeta_2}$ ,  $M\alpha\beta$ ,  $M\gamma$ , and  $M_2-N_4$  (also labeled with  $M_1-N_2$  and  $M_3-O_4$ ) which are discussed in the text.

The target thickness dependence was determined for  $^{79}\text{Au}$  and  $^{82}\text{Pb}$  for incident  $^{19}\text{F}^{q+}$  ions. The region of thickness, where M-shell x-ray production cross sections were essentially independent of the target thickness, was used for the projectile charge state dependent studies. The thicknesses of the targets used were  $^{79}\text{Au}$  ( $4.2 \mu\text{g}/\text{cm}^2$ ),  $^{82}\text{Pb}$  ( $12.5 \mu\text{g}/\text{cm}^2$ ),  $^{83}\text{Bi}$  ( $9.6 \mu\text{g}/\text{cm}^2$ ),  $^{92}\text{U}$  ( $3.5 \mu\text{g}/\text{cm}^2$ ).

### Results and Discussions

In Fig. 2, the variation of a ratio of the x-ray yield to the Rutherford yield with the charge state  $q$  of  $^{19}\text{F}^{q+}$  ion is plotted for various resolved peaks (see Fig. 1)  $M_{\zeta_1\zeta_2}$ ,  $M\alpha\beta$ ,  $M\gamma$ ,  $M_2-N_4$  and for the sum peaks of  $M\alpha\beta\gamma$  and total M. Within the experimental uncertainties, all of the ratios point toward a trend. The ratio for a particular peak at  $q=9$  is larger than a ratio for the same peak at  $q=8$ , which in turn, is larger than the average of the ratio, for the same peak, at  $q=4,5,6$ . Further, the observed ratios, for any peak, are essentially independent of the projectile charge state for  $q=4,5,6$ . The charge state  $q=9$  for  $\text{F}^{q+}$  corresponds to a completely stripped nuclei, while  $q=8$  corresponds to a hydrogen-like atom.

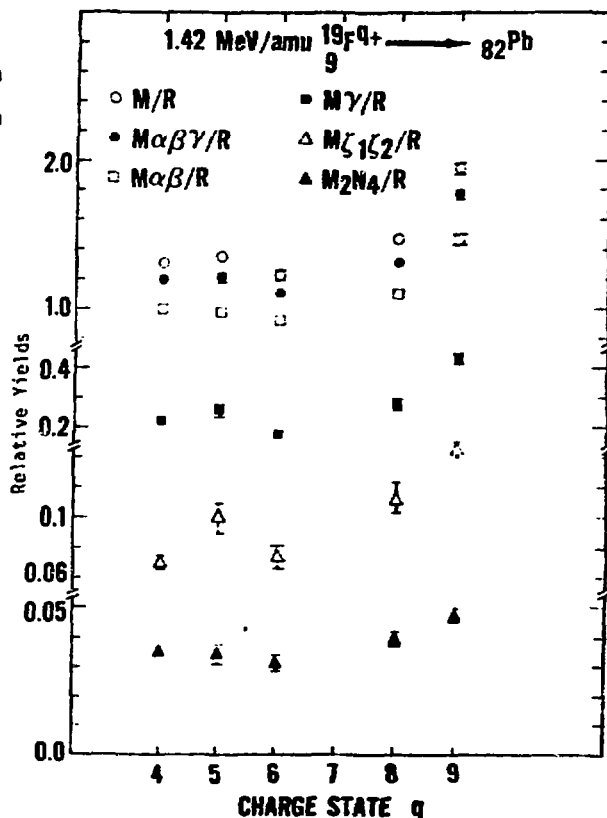


Fig. 2. A plot of the ratio of the M-shell x-ray yield to the Rutherford yield  $R$  versus the charge state  $q$  of the incident 1.42 MeV/amu  $^{19}\text{F}^{q+}$  ion is shown. Individual M-shell x-ray peak ratios with the Rutherford yields  $R$  are shown by various symbols. For example, open circle represents the ratio for total M-shell x-ray yield with the Rutherford yield, while a closed circle is for ratio of  $M\alpha\beta\gamma$  x-ray yield with  $R$ .

In Fig. 3, an average of target M-shell x-ray production cross section, for projectile charge states  $q=4,5,6$  of  ${}^{19}\text{F}^{q+}$  is plotted versus  $Z_1/Z_2$ .  $Z_1$  and  $Z_2$  are the atomic numbers of the projectile and target respectively. This average target M-shell x-ray production cross section corresponds to a sum of DI and electron capture to L, M and higher shells of the projectile. The dashed curve represents the DI calculation in the PWBA and includes no capture to any shells. The apparent good agreement between the experimental data and the PWBA theory may be fortuitous or it may indicate that EC to the L-, M- and higher shells is not a large contributor to target M-shell ionization at these energies and for these values of  $Z_1/Z_2 = 0.098$  to  $0.114$  in the present experiment. The rather constant values of the ratio of x-ray to scattered particle yields in Fig. 2 for different numbers of L-shell vacancies ( $q=4,5,6$ ) supports the latter explanation.

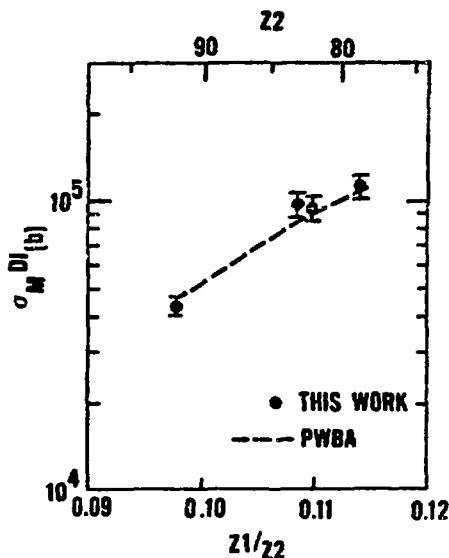


Fig. 3. The average target M-shell x-ray production cross section  $\sigma_M^{\text{DI}}$  for incident  ${}^{19}\text{F}^{q+}$  ions with  $q=4,5,6$  is plotted versus  $Z_1/Z_2$ . The DI calculation of PWBA is shown by the dashed curve.

The M-shell to K-shell EC cross sections are inferred by comparing the target M-shell x-ray production cross sections for the incident projectile with one or two K-shell vacancies, with the target M-shell x-ray production cross section for the incident projectile with no K- vacancies ( $q=4,5,6$ ).

The theoretical M-shell to K-shell EC cross sections are determined by calculating them in OBK-N<sup>2</sup> approximation for each of the initial orbital angular momentum states in the target M-shell. The final states are comprised of the K-shell of the projectile.

The theoretical M-shell to K-shell EC cross section is converted to an x-ray production cross section by using the fluorescence yield for each subshell<sup>19,20</sup> and the transition probabilities for transitions within the M-shell<sup>19</sup>. The EC cross sections, for one and two K-shell vacancies in the projectile, are inferred as previously outlined.

In Fig. 4,  $\sigma_M^{\text{EC}}$  which represents the inferred target M-shell x-ray production cross section due to the EC to the K-shell of the projectile  ${}^{19}\text{F}^{q+}$  with 1 K-shell vacancy ( $q=8$ ) and 2 K-shell vacancy ( $q=9$ ) is plotted versus  $Z_1/Z_2$ . OBK-N calculations of the x-ray produc-

tion cross sections, plotted as a dashed curve, overestimate the experimentally inferred cross sections by more than an order of magnitude. Both the experimental data points and the theory show an increasing cross section with decreasing  $Z_2$  as expected.

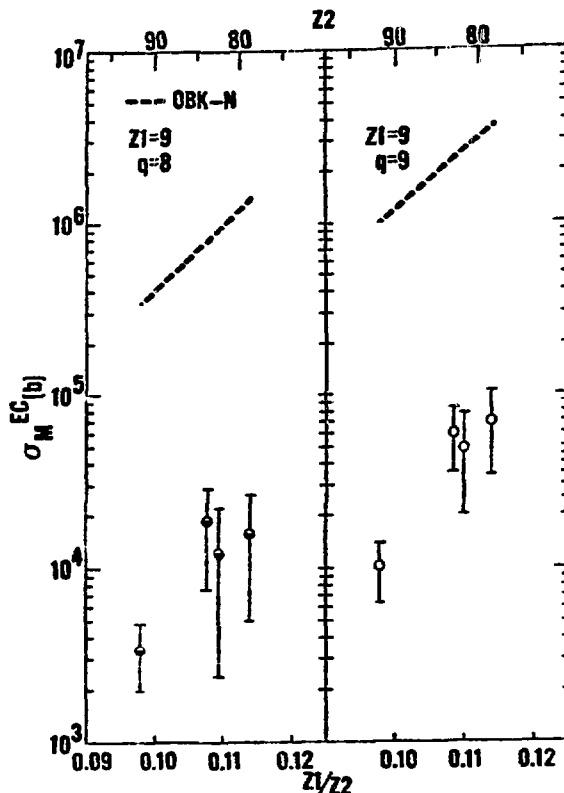


Fig. 4. The inferred target ( $Z_2$ ) M-shell to projectile K-shell x-ray production cross section  $\sigma_M^{\text{EC}}$  due to EC for 1 K-shell vacancy ( $q=8$ ) and 2 K-shell vacancies ( $q=9$ ) present in the projectile ( $Z_1$ ) are plotted versus  $Z_1/Z_2$ . Theoretical prediction of EC cross section in OBK-N calculations are shown by a dashed curve. The targets used are  ${}^{79}\text{Au}$ ,  ${}^{82}\text{Pb}$ ,  ${}^{83}\text{Bi}$  and  ${}^{92}\text{U}$ . The half-filled circles represent data for hydrogen-like ( $q=8$ ) Fluorine ions and the open circles represent data for fully stripped ( $q=9$ ) Fluorine ions.

#### Conclusions

M-shell x-ray production cross sections of  ${}^{79}\text{Au}$ ,  ${}^{82}\text{Pb}$ ,  ${}^{83}\text{Bi}$  and  ${}^{92}\text{U}$  were measured for incident  $1.42 \text{ MeV}/\text{amu}$   ${}^{19}\text{F}^{q+}$  ions, with charge states of  $q=4,5,6,8,9$ . These cross sections were found to be independent of the projectile charge state  $q$  for  $q=4,5$  and  $6$ .

The ratio of M-shell x-ray yields with the Rutherford yields are seen to be enhanced for cases of  ${}^{19}\text{F}$  ions with one or two K-shell vacancies. This can be attributed to the formation of target M-shell vacancies via the electron capture from the M-shell of the target into the K-shell of the projectile.

The ratios of M-shell x-ray yields with the Rutherford yields is seen to be constant for cases of  ${}^{19}\text{F}$  ions with no K-shell vacancies and 5,6,7 L-shell vacancies. This, together with the good agreement between the target M-shell direct ionization data and the DI calculation in the PWBA theory indicates that the EC to the L, M and higher shells is not a large contributor to the target M-shell ionization.

The x-ray production cross section attributed to EC were determined by subtracting the average of the projectile charge state independent data from the hydrogen-like ( $q=Z_1-1$ ) or fully stripped ( $q=Z_1$ ) projectile data. The comparison of the inferred EC cross section data with that determined from OBK-N approximation shows that the theory overestimates the data by more than an order of magnitude for all of the data. This disagreement of the OBK-N with experimental data is consistent with conclusions of similar work done for K and L shells<sup>9,17</sup>.

#### References

1. B. -H. Choi, Phys. Rev. A 7, 2056 (1973).
2. J.M. Hansteen, O.M. Johnson and L. Kocbach, At. Data and Nucl. Data Tables 15, 305 (1975).
3. D.E. Johnson, G. Basbas and F.D. McDaniel, At. Data and Nucl. Data Tables 24, 1 (1979).
4. J.R. Oppenheimer, Phys. Rev. 31, 349 (1928).
5. H.C. Brinkman and H.A. Kramers, Proc. Acad. Sci. (Amsterdam) 33, 973 (1930).
6. V.S. Nikolaev, Zh. Eksp. Teor. Fiz. 51, 1263 (1966) [Sov. Phys. -JETP 24, 847 (1967)].
7. E. Merzbacher and H.W. Lewis, Encyclopedia of Physics, edited by S. Flugge (Springer-Verlag, Berlin, 1958) Vol. 34, p. 166.
8. G. Basbas, W. Brandt and R. Laubert, Phys. Rev. A 17, 1655 (1978), Phys. Rev. A 7, 983 (1973).
9. F.D. McDaniel, J.L. Duggan, G. Basbas, P.D. Miller and G. Lapicki, Phys. Rev. A 16, 1375 (1977).
10. J.F. Reading, A.L. Ford, G.L. Swatford and A. Fitchard, Phys. Rev. A 20, 130 (1979).
11. C.D. Lin, S.C. Soong and L.H. Tunnell, Phys. Rev. A 17, 1646 (1978).
12. G. Lapicki and W. Losonsky, Phys. Rev. A 15, 896 (1977).
13. G. Lapicki and F.D. McDaniel, Phys. Rev. A 22, 1896 (1980).
14. F.T. Chan and J. Eichler, Phys. Rev. Lett. 42, 58 (1979); Phys. Rev. A 20, 104 (1979); Phys. Rev. A 20, 1841 (1979).
15. R. Shakeshaft, Phys. Rev. A 17, 1011 (1978); Phys. Rev. A 20, 779 (1979); R. Shakeshaft and L. Spruch Rev. Mod. Phys. 51, 369 (1979).
16. T.J. Gray, P. Richard, G. Gealy and J. Newcomb, Phys. Rev. A 19, 1424 (1979); R.K. Gardner, T.J. Gray, P. Richard, C. Schmiedekamp, K.A. Jamison and J.M. Hall, *ibid.* 19, 1896 (1979); A. Schmiedekamp, T.J. Gray, B.L. Doyle and U. Schiebel, *ibid.* 19, 2167 (1979).
17. F.D. McDaniel, A. Toten, R.S. Peterson, J.L. Duggan, S.R. Wilson and J.D. Gressett, P.D. Miller and G. Lapicki, Phys. Rev. A 19, 1517 (1979).
18. W.J. Gallagher and S.J. Cippola, Nucl. Inst. & Meth. 122 (1974) 405.
19. E.J. McGuire, Phys. Rev. A 5, 1043 (1972).
20. W. Bambynek, B. Craseman, R.W. Fink, H.U. Freund, H. Mark, C.D. Swift, R.E. Price, P.V. Rao, Rev. Mod. Phys. 44, 716 (1972).